INDUCED RADIOACTIVITY AND RELATED MEASUREMENTS IN A 3 GeV HIGH CURRENT PROTON SYNCHROTRON

M. Awschalom, F. L. Larsen, W. Schimmerling
Princeton-Pennsylvania Accelerator
Princeton University, Princeton, New Jersey

Some of the experience gained while working with and around the radioactivated components of a high current 3 GeV proton synchrotron is briefly presented and discussed. The topics presented are: 1) air radioactivation in the synchrotron room, 2) correlation between measured neutron fluxes through the synchrotron magnets and remanent radioactivity, 3) transferrable radioactivity, 4) radiation exposure to personnel, 5) radioactivation of machine components and shielding.

Air Radioactivation

We have previously reported on the existence of radioactive gases near our target section[1]. It was then established that the main components were O^{14}, O^{15}, N^{13}, C^{11}. However, further information has been obtained.

For the calculations that follow we have assumed that the atmospheric composition is 0.78 N_2, 0.21 O_2 and almost .01 Ar, by volume. Thus, the Ar atomic-concentration is a factor of 50 lower than either oxygen or nitrogen. We irradiated an Argon-sample one meter downstream from the meson target at 15°. Gamma ray analysis of the sample showed the existence of the following isotopes: Na^{24}, Mg^{27}, Al^{28}, Al^{29}, S^{37}, Cl^{34}, Cl^{38}, Cl^{39}, and Ar^{41}. The total nonelastic cross-section of argon is presumably 1.8 higher for Ar than for O. We will therefore, in the following, ignore the radioactive products from Ar. Further analysis of the Ar-spallation products is in progress. Thus, we studied the spallation products from oxygen and nitrogen, whose most important products in our case are O^{14}, O^{15}, N^{13}, C^{11}. We used distilled water as an oxygen sample and NH_4NO_3 as a practical nitrogen sample. The atomic composition of atmospheric air is then 2.78 x NH_4NO_3-1.92 x H_2O.

All the isotopes in question are positron-emitters. Therefore, we decided to separate them by measuring the time-decay of the annihilation-peak. We used a 3" x 3" NaI(Tl) well crystal and suitably fast and stable electronics. Finally, the intensities of the different components were obtained by a least-squares analysis of the multidecay curve.

In order to increase the accuracy of the unfolding of the multidecay curve, a good knowledge of the half-lives present is essential. Therefore, we undertook an accurate determination of the half-life of C^{11}. The result of this determination is $T_{1/2}$= 20.39 ± .04 min. for C^{11}.

Table I shows the measured and calculated saturation activities per cm^3 of air at 70 cm and 70 degrees from the meson target, normalized to 10^{12} protons/sec on a 3.8 cm Pt-target. The uncertainties are statistical only. A_{av} are average concentrations throughout the machine as explained below.

Table I

Isotope	$T_{1/2}$(Min.)	$A(\mu Ci/cm^3)$	$A_{av}(\mu Ci/cm^3)$
O^{14}	1.3	$(.8\pm1.8)\times10^{-5}$	4×10^{-8}
O^{15}	2.1	$(1.20\pm.13)\times10^{-4}$	6.5×10^{-7}
N^{13}	10.1	$(.97\pm.02)\times10^{-4}$	5.3×10^{-7}
C^{11}	20.39	$(1.04\pm.01)\times10^{-4}$	5.7×10^{-7}

Let $A(r,\theta)$ be the activity of an isotope per unit volume of atmospheric air, at (r,θ), irradiated by secondaries from the above meson target. The average activity $\bar{A}$ in any volume may be evaluated if a functional dependence of A is known.

Samples of aluminum and polyethlene were irradiated for about 20 days around the meson target in order to estimate the θ dependence of $A(r,\theta)$. It can be seen from figure 1 that this function may be approximated by:

$$A(r,\theta) = b \exp(-a\theta)$$

Table II shows the results of a least-squares fitting of the data-points with a straight line.

Table II

Reaction	$a(rad^{-1})$
Be^7 from C^{12}	1.92
C^{11} from C^{12}	1.75
Na^{22} from Al^{27}	1.54
Na^{24} from Al^{27}	1.08

Figure 2 shows the results of measurements of air flow in the synchrotron room. Neglecting turbulence, we assume the air in the synchrotron room to circulate with an average speed of

50 ft./min., reaching the target area again in T = 5 min., that all irradiation takes place within the sphere shown, that the air on the average spends Δt = 10 sec in this region and that the airflow is confined by the columns and the outer wall.

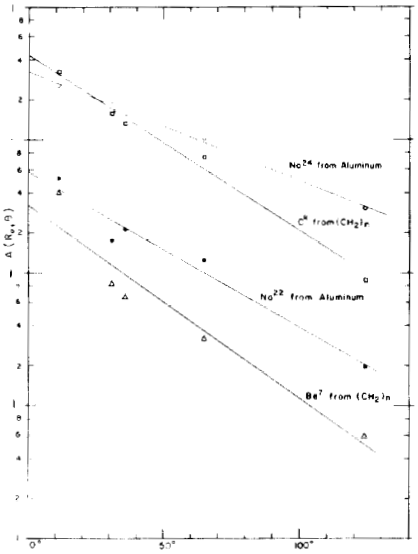

Fig. 1. Distribution of induced radioactivity in Al and C samples around a 38 mm Pt-target, as a function of angle. Angle measured with respect to the direction of the incoming protons.

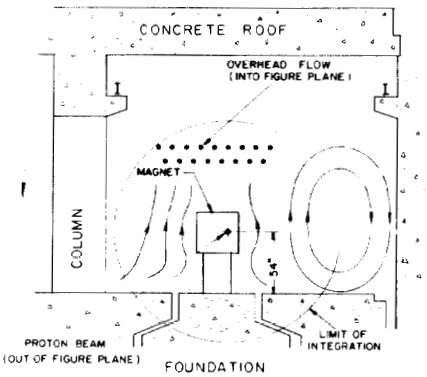

Fig. 2. Air flow in the synchrotron room. Air speeds are approximately 40-60 ft/min. The air flow alongside the magnets is inclined 50 degr. into the plane of the figure.

The concentrations near the target section after the air has circulated N times around the machine is then:

$$A \sim \overline{A}\,[1-\exp(-\lambda\,\Delta t)] \;/\; [1-\exp(-\lambda\,T)]$$

Where λ is the decay-constant.

Let A(x) be the concentration in a location whose distance from the target is x along the direction of the airflow, and P the pathlength of a full revolution.

$$A(x) = A \exp(-\lambda\, Tx/P)$$

The average concentration A_{av} the outer ring is then

$$A_{av} = P^{-1} \int_0^P A(x)\, dx \sim \overline{A}\,\Delta t/T$$

If then, we choose a =1.75 rad.$^{-1}$ for all isotopes and take into consideration the shadowing by the magnets, we get the results shown in Table I.

These concentrations should be compared to[2] $(MPC)_a = 2\times10^{-6}$ μCi/cm^3 for 40 hours occupational exposure for N^{13} and O^{15}. If the $(MPC)_a$ for C^{11} is comparable to that of N^{13} and O^{15}, we may conclude that with a beam intensity of 10^{12} protons/second on a 38mm Pt target, our concentration of radioactive gases is not a personnel problem.

Neutron Fluxes and Remanent Radioactivity of the Synchrotron

The neutron flux through the top center of all synchrotron magnets has been monitored from the first day attempts were made to accelerate protons. For this purpose we have used neutron flux integrators of the type described by A. R. Smith[3] whose calibration we have rechecked. Our present knowledge of the composition of the particle fluxes at those locations does not warrant a more sophisticated method of integration. This neutron flux is expected to correlate well with the remanent radioactivity of the synchrotron proper. On figure 3, the solid squares show the neutron flux for the period 12/7/66 to 1/3/67.

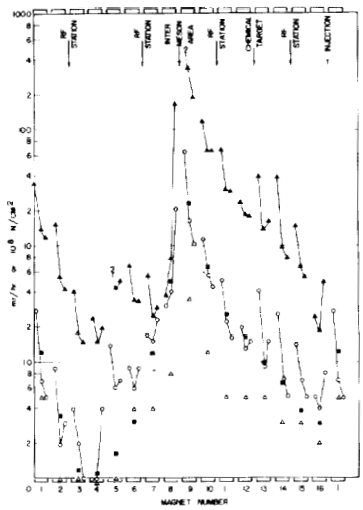

Fig. 3. Correlation between neutron flux and remanent radioactivity. Solid squares: neutron flux. Solid triangles: vacuum chamber front spacers, 34 hr cooling time. Open circles: magnet top centers, 34 hr cooling time. Open triangles: magnet top centers, 52 day cooling time.

This distribution is essentially the same as that for the entire period from 4/15/63 to 1/3/67 except for a scale factor. The solid triangles show the exposure dose rate measured with an ionization chamber on contact with the outside of the vacuum chamber, after a thirty-four hour cooling period (one weekend). The open circles show the same type of measurements after the same cooling time but on top of the synchrotron magnets. The open triangles are those of a survey made at the top center of the magnets after a fifty-two day cooling period. These curves show an excellent correlation with one another and with what one would expect from the use of a thick meson producing target (38 mm Pt) upstream from magnet number nine, see Fig. 4. The higher spatial resolution of the open circle and solid triangle data allows for the identification of those structures which scrape the beam such as RF drift tubes, inflector, etc. The use of neutron flux monitors as diagnostic tools in the early days of operation demonstrated the loss of protons "over the top" of the magnetic field, when excessive numbers of protons struck the inflector. Ionization chambers have been used for the same purpose.

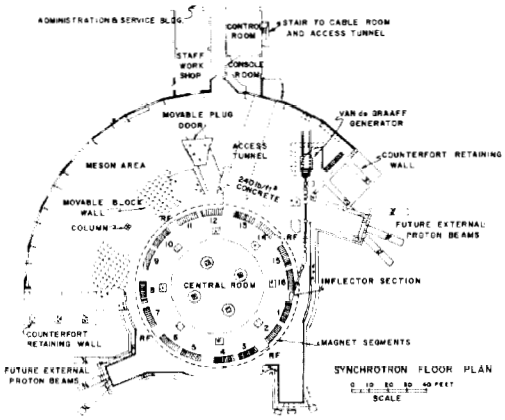

Fig. 4. Floor plan of the synchrotron and immediate facilities.

Figure 5 shows the dose rate at different azimuthal and radial positions between the magnets and the shielding wall. In general, the dose rates fall off as the distance from the magnet increases. All data points were taken with air filled ionization chambers. The solid lines represent the average of two sets of points taken within fifteen minutes of each other. The curves have been normalized arbitrarily to improve legibility. The anomalous shape of the curve for magnet seven is due to the fact that the ionization chamber was able to "see" the meson target more and more as the distance from magnet seven increased.

The magnet eleven location was further studied with two ionization chambers measuring simultaneously the dose rate for approximately thirty two hours from about half an hour after machine turn-off. These air filled ionization chambers were located at 30cm from the vacuum chamber and 15cm from the wall. They were somewhat isolated from the rest of the synchrotron room by lead curtains sixty-four mm thick. Figure 6 shows that the dose rate from the synchrotron was three times larger than that of the wall initially and that this ratio increased in time.

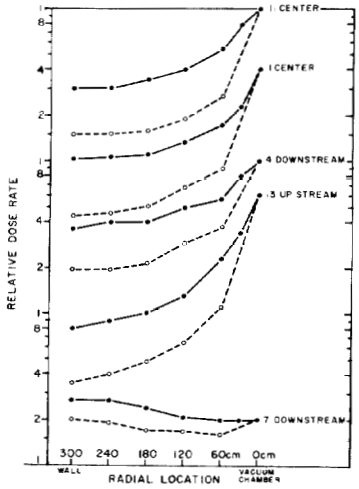

Fig. 5. Exposure dose rates between magnets & walls, on median plane. The data have been arbitrarily normalized to improve legibility and emphasize relative wall contribution. Solid lines: data gathered within one half hour of machine turn-off. Dashed lines: similar survey thirty-four hours later.

The skyshine contribution was slightly less than 10%. Surveys made at other times show that the wall is essentially a plane source. The magnet, as a radiation source, is more difficult to describe. It may be regarded as a plane cource plus a bump in the middle. Figure 5 shows negligible change in the dose rate versus distance from 120 to 300 cm at the two times. This is in qualitative agreement with the source geometry. Since the dose rate from the wall is about one third that of the magnet, soon after machine turn-off, one could see that there might be some advantage in the addition of boron to the concrete of the walls to reduce the Na^{24} contribution[4].

Transferable Radioactivity

Wipe tests of radioactive materials are regularly made to ascertain the presence of transferable radioactivity. The results of these wipe tests have generally been negative. The only one exception has been the molybdenum sesquisulfide power used as lubricant and corrosion preventive. This powder was found to be quite radioactive and was replaced by lithium grease.

Radiation Exposure to Personnel

The excellently designed shielding around the accelerator has resulted in freedon from skyshine and groundshine. Thus, doses to personnel working outside the central room of the synchrotron are essentially background except for very few instances. Consequently, our only problem in personnel exposure control has been gamma doses from the radioactivated synchrotron components.

Figures 7 and 8 show the cumulative personnel dose distributions plotted on lognormal probability paper.[5] The results in figure 7 are quarterly gamma exposures for all monitored personnel and in figure 8, exclusively for personnel receiving non-zero doses. The median values x(1/2, Q) have been indicated for the Q-th quarter, the most probable value being approximately zero on all curves in figure 7.

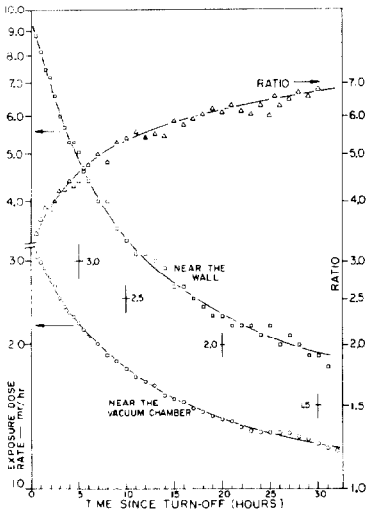

Fig. 6. Exposure dose rates near synchrotron magnet eleven and corresponding point on shield wall. Measurements made on median plane with air filled ionization chambers which were located at 15 cm from the wall and at 30 cm from the front spacer of the vacuum chamber. These ion chambers were partly screened from the room background with lead cutrains 64 mm thick. Note the change in scale in the ordinates.

It should be noted that ninety-five percent of the personnel monitored received gamma doses of less than 1 rem/quarter. In very few instances have neutron or beta doses been recorded in excess of 100 mrem. It may be argued that the low neutron doses recorded are due to the inherent limitations of the film badges,[6] but even the suggested correction factor of four for the recorded neutron doses would keep these exposures very low.

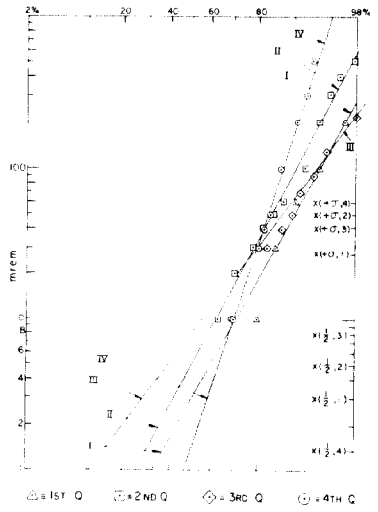

Fig. 7. Cumulative quarterly gamma dose, zero doses included, monitored by film badges in 1966.

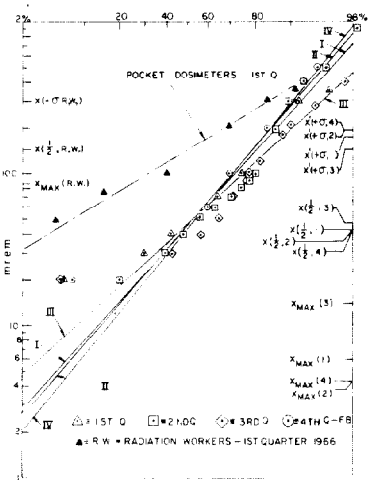

Fig. 8. Cumulative quarterly non-zero gamma doses, monitored by film badges in 1966. Pocket dosimeter results in the first quarter are shown for comparison.

Radioactivation of Machine Components and Shielding

Information concerning the radioactivation of machine components is essential for planning maintenance and repair within conservative limitations on the dose received by personnel. The components requiring most attention are the synchrotron vacuum chambers, which are replaced and reconstructed on a regular basis at PPA.

The decay of several such vacuum chambers has been followed for some time. The chambers are monitored at several positions with a

portable ionization chamber. The results of measurements at two positions are plotted versus time in figure 9 for vacuum chamber number 9-15.

The vacuum chambers are made of an alloy containing 70 percent Cu and 30 percent Ni. Reaction products with comparable half-life are Fe^{59} (45 days), Co^{56} (77 days) and Co^{58} (71 days).

Very little activation of shielding materials has been found. The dose due to large shielding blocks moved during shutdowns has been found to be less than 10 mrad/hr @ 1 ft. except in very few instances. To measure the radioactivity of smaller shielding blocks (e.g. lead bricks) a hole is generally left when laying the bricks upon a skid and the exposure is measured inside and outside. Few radioactive bricks have been found.

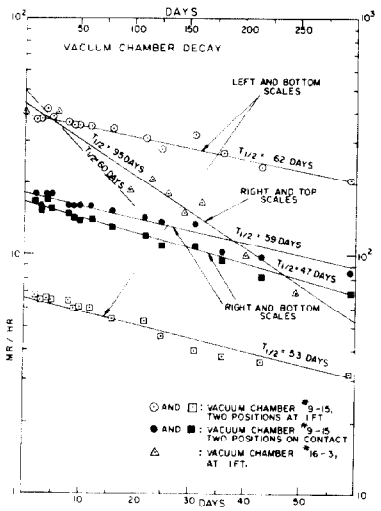

Fig. 9. Exposure dose rate decay of a vacuum chamber.

No long lived activity has been found in the water used to cool the magnets. This is mainly due to the efficiency of the ion exchange columns. Traces of Be^{7} were found in the oil used for cooling at the RF stations. These, however, are of the order of 10^{-10} Ci per cm^3 and thus quite negligible.

References

1. M. Awschalom, F. L. Larsen & R. E. Sass, "The Radiations Measurements Group at the Princeton-Pennsylvania 3 GeV Proton Synchrotron" Proc. USAEC First Symp. on Accel. Rad. Dosim. & Exp., 57-79 CONF-651109(Nov 3-5, 1965)

2. J. E. Russel & R. M. Ryan, "Radioactive Gas Production From the R.P.I. Electron Linear Accelerator", IEEE Trans. Nucl. Sci. NS-12(3), 678-682(1965)

3. A. R. Smith, "A Cobalt Neutron-Flux Integrator", Health Physics 7, 40-47 (1961)

4. D. Nachtigall & S. Charalambus, "Induced Na^{24} Activity In the Concrete Shielding of High Energy Accelerators", CERN Report 66-28 (September 16, 1966)

5. W. Schimmerling & R. E. Sass, "Experience with Commercial Film Badge Service", Report PPAD 611-E (1967)

6. H. J. Gale, "The Lognormal Distribution and Some Examples of its Application in the Field of Radiation Protection", Report AERE-R4736 (1965)